Bimodal Distribution of Nuclear Factor-κB Activation and Expression of Subunits in Experimental Models of Intracerebral Hemorrhage In Vivo

Ze-Li Zhang, MD,* Yan Song, MD,† Feng Li, MD,† and Qi-Bing Huang, MD*

Objective: The exact role of nuclear factor-kappaB (NF-κB) in intracerebral hemorrhage (ICH) is still unclear to date. The aim of the present study is to clarify the activation of NF-κB and the role of its subunits in inflammatory response and cell death after ICH. *Methods*: The model of ICH rats was made, and at preset time points after operation, as well as rats in the control and sham groups, the ipsilateral striatum and tissue around was obtained for detection of NF-κB activation, cell death, and expression of interleukin-1β, tumor necrosis factor-α, Caspase-3, Bcl-2, and NF-κB subunits. *Results*: There were 2 peaks of NF-κB activation (2 days and 10 days) after ICH. The expression of p50 and p65 reached the peak at 1 day and 2 day, leading to the first peak of NF-κB activation, and that of c-Rel at 10 day, leading to the second. The peak of cell death and caspase-3 expression, and the nadir of bcl-2 expression appeared to be synchronizing with or right after the first peak of NF-κB activation. Then, at the second peak of NF-κB activation, cell death, and caspase-3 expression decreased and the bcl-2 expression returned to the normal level. *Conclusions*: NF-κB activation showed a bimodal distribution mode after ICH. We can speculate that p50 and p65 may promote the inflammatory response and apoptosis, and c-Rel may play the opposite role. Measures might be performed at the different phases to reduce the brain injury in the early stage and promote the brain recovery in the late stage after ICH.

Key Words: Intracerebral hemorrhage—nuclear factor-kappaB—bimodal distribution—inflammatory response—cell death

Introduction

As a frequent form of cerebrovascular diseases, primary intracerebral hemorrhage (ICH) accounts for 30% of all cases of stroke in China, more than twice the number in the West.[1-4] It is the leading cause of stroke related mortality and morbidity worldwide, which is higher than that of ischemic stroke. Forty percent of ICH patients will die during the first month after ICH, and functional outcome in survivors is also poor with less than 20% being able to live independently at 6 months.[5]

A series of inflammatory response in brain tissue arise after ICH.[6] Nuclear factor-κB (NF-κB) has been recognized as a critical regulator of inflammatory responses since its discovery.[7,8] In unstimulated cells, inactive NF-κB is sequestered in the cytoplasm by inhibitory protein IκB (inhibitor of NF-κB). When ICH occurs, NF-κB can be activated by a series of factors such as thrombin, tumor

Abbreviations: ICH, intracerebral hemorrhage; NF-κB, nuclear factor-kappaB; IL-1β, interleukin-1β; TNF-α, tumor necrosis factor-α; SAH, subarachnoid hemorrhage; HI, hypoxia ischemia; TBI, traumatic brain injury; EMSA, electrophoretic mobility shift assay; TUNEL, terminal deoxynucleotidyl transferase-mediated dUTP-biotin nick end labeling

From the *Department of Neurosurgical Intensive Care Unit, Qilu Hospital of Shandong University and Brain Science Research Institute of Shandong University, Jinan, Shandong Province, China; and †Department of Neurosurgery, Qilu Hospital of Shandong University and Brain Science Research Institute of Shandong University, Jinan, Shandong Province, China.

Received September 22, 2018; revision received November 12, 2018; accepted November 29, 2018.

Financial Disclosure: This study is supported by National Natural Science Foundation of China (81501054).

Address correspondence to Qi-Bing Huang, MD, Department of Neurosurgical Intensive Care Unit, Qilu Hospital of Shandong University and Brain Science Research Institute of Shandong University, Jinan 250012, Shandong Province, China. E-mail: cnyuguangliu@163.com.

1052-3057/$ - see front matter

https://doi.org/10.1016/j.jstrokecerebrovasdis.2018.11.028

necrosis factor-α (TNF-α), interleukin-1 (IL-1), etc.[9-12] After activation, the free NF-κB rapidly migrates into the nucleus, binds to DNA, and promotes the transcription of genes for the release of proinflammatory substances. The activation of NF-κB is also closely related to the cell apoptosis. Therefore, NF-κB plays a major role in the inflammatory response after ICH.[4,13]

The close relationship between NF-κB activation and cell death after ICH seems obvious. However, it is still questionable whether NF-κB activation promotes cell death or it is a compensatory mechanism to promote cell survival. Recently, studies have indicated a dual role of NF-κB during regulation of neuron survival in pathological conditions, impacting like a double-edged sword on both brain damage and neuroprotection, which are associated with different subunits.[14,15] Studies have shown that there are double peaks of cerebral NF-κB activity after subarachnoid hemorrhage (SAH), neonatal hypoxia-ischemia (HI) and traumatic brain injury (TBI), which are also associated with different subunits.[16,17] Further studies have shown that early NF-κB activation contributes to brain damage, and late NF-κB provides neuroprotection and upregulates antiapoptotic molecules.[16]

Whether NF-κB has the similar double-peak activation after ICH associating with different subunits? Is the apoptosis of perihematomal brain cells related to the expression of different subunits? Until now, these questions stay unanswered as there is still no relevant research. In the present study, the model of ICH rats was made, the activation of NF-κB, expression of its subunits, apoptosis-related factors, and the apoptotic cell death of perihematomal brain cells were detected in experimental models of ICH in vivo. The results were analyzed to clarify these issues above.

Materials and Methods

ICH Model

Male Wistar rats (n = 80, 14-16 weeks), weighing from 240 to 260 g were provided by the Laboratory Animal Center of Shandong University. They were kept in a temperature-controlled environment (21°C) on a 12 hours light-dark cycle with free access to water and food. Experimental ICH was induced by the stereotaxic intrastriatal administration of bacterial collagenase type IV (Solarbio, Beijing, China) as previously described.[18,19] In brief, after anaesthetized with 10% chloral hydrate by intraperitoneal injection (3 mL/kg), rats were placed on a stereotaxic apparatus (Zhongshi Dichuang, Beijing, China). An incision was made in the middle of the scalp and a burr hole was made by a dental drill. Then a microsyringe (Gaoge, Shanghai, China) was stereotaxically implanted through the hole into the right striatum (coordinates: 0.2 mm posterior to bregma, 6.0 mm below the skull, and 3.0 mm right to the middle line). ICH was induced via administration of 1 μL saline containing 0.23 U bacterial collagenase type IV over a 5-minute period. In order to avoid backflow, the microsyringe was kept in situ for another 10 minutes before being slowly withdrawn. After collagenase infusion, craniotomies were sealed with bone wax, and wounds were sutured. Sham ICH was induced with a stereotaxic needle insertion and an injection of equal volume (1 μL) of saline instead of collagenase. Nothing was performed for the rats in the control group (Ctrl group). Rectal temperature was maintained at 37 ± 0.5°C using a thermistor-controlled heating blanket.

Animal welfare and experimental procedures were in accordance with the Care and Use of Laboratory Animals (National Research Council, Washington DC). The study protocol was approved by the ethics committee of the hospital.

Tissue Preparation

At defined time points, ie, 6 hour, 12 hour, 1 day, 2 day, 4 day, 7 day, 10 day, and 14 day after operation, rats were reanesthetized with 10% chloral hydrate by intraperitoneal injection. Rats were sacrificed by transcardiac perfusion with cold Phosphate Buffered Saline (PBS) to eliminate the RNA and protein expressed by blood cells. Brains were then dissected on ice immediately to obtain half of the ipsilateral striatum, which was flash-frozen in liquid nitrogen and stored at −80°C for molecular biology experiments. Then the other half of the ipsilateral striatum and the tissue around was removed carefully and kept in 4% paraformaldehyde at 4°C for fixation of 3 days. After fixation, they were paraffin embedded and processed to 5 μm sections for morphology study.

Electrophoretic Mobility Shift Assay (EMSA)

In brief, the nucleoprotein was extracted from the brain tissue according to the instructions provided by the manufacturer (The Thermo Fisher Scientific Inc.). Protein concentrations were determined by using a Micro BCA Protein Assay Kit (Thermo Fisher Scientific Inc.). Half of the nucleoprotein was stored at −80°C for electrophoretic mobility shift assay (EMSA), and the other half for Western blotting. LightShift Chemiluminescent EMSA Kit (Thermo Scientific, 20148) was used for EMSA. 5′-Biotin-labeled NF-κB oligo 5′-AGTTGAGGGGACTTTCCCAGGC-3′ was used as the probe. EMSA was performed according to the manufacturer's instructions. At last, all immunoblots were visualized and analyzed using fully automated chemiluminescence imaging analysis system (Tanon 5200, China) with associated software.

Western Blotting

The extracted nucleoprotein samples described previously were boiled for 10 minutes, loaded onto 14% SDS-PAGE gel, and electrophoresis was run for 2 hours. Protein was electrophoretically transferred onto 0.22 m

nitrocellulose and immunoblotted with the primary antibody of NF-κB p50 (13586 rabbit monoclonal, CST), NF-κB p65 (ab19870 rabbit polyclonal, Abcam), NF-κB c-Rel (12707 rabbit monoclonal, CST), Lamin A, respectively, and then the secondary antibody (Peroxidase-AffiniPure Goat Anti-Rabbit IgG (H+L), Jackson ImmunoResearch).

The total protein was extracted by lysing the prepared tissue at 4°C for 30 minutes in lysis buffer (20 mM tris (hydroxymethyl) aminomethane-HCl, pH 7.5, 140 mM NaCl, 1 mM ethylenediaminetetraacetic acid, 50 U/mL aprotinin, 1 mM phenylmethylsulphonyl fluoride, and 1 mM sodium orthovanadate) containing 1% Nonidet P-40 detergent. Protein concentrations were determined by using Micro BCA Protein Assay Kit (Thermo Fisher Scientific Inc.). The total protein samples were boiled for 10 minutes, loaded onto 14% SDS-PAGE gel, and electrophoresis was run for 2 hours. Proteins were electrophoretically transferred onto 0.22 m nitrocellulose and immunoblotted with primary antibodies of IL-1β (ab9787, rabbit polyclonal, Abcam), TNF-α (ab9755 rabbit polyclonal, Abcam), Caspase-3 (9665 rabbit monoclonal, CST), Bcl-2 (ab59348 rabbit polyclonal, Abcam), -actin, respectively, and then the secondary antibody (Peroxidase-AffiniPure Goat Anti-Rabbit IgG (H+L), Jackson ImmunoResearch).

All immunoblots were visualized and analyzed using fully automated chemiluminescence imaging analysis system (Tanon 5200, China) with associated software.

Terminal Deoxynucleotidyl Transferase-Mediated dUTP-Biotin Nick End Labeling (TUNEL) Assay

DNA fragment was detected with the terminal deoxynucleotidyl transferase-mediated dUTP-biotin nick end labeling (TUNEL) assay. Tissue sections were deparaffinized and hydrated, and then TUNEL assay was performed according to the instructions provided by the manufacturer (In Situ Cell Death Detection Kit, POD, Roche, Germany). The samples were incubated in the TUNEL reaction mixture and rinsed with PBS. Then after being incubated in the diaminobenzidine (DAB) substrate solution, rinsed and mounted under glass cover slip, the slide was analyzed under light microscope by 3 professors of pathology in a blinded fashion. A total of 5 no-repeat fields (400× high magnification) were randomly selected, the TUNEL positive cells were identified, and the numbers of positive cells in all of the 5 fields were added up as the result. The results recorded by the 3 pathologists were consistent.

Statistical Analysis

SPSS 19.0 statistical analysis software and Excel 2016 were used in the statistical analysis and charting. The normally distributed continuous variables were expressed as mean ± standard derivation, and the categorical variables were showed as n (%). The normally distributed continuous variables were analyzed with Student's *t* test, and categorical variables with chi-square test. Statistical significance was set at *P* less than .05.

Results

ICH Model

There was no death due to ICH in all groups. The hemorrhage was located in the basal ganglia and the homogeneity of hematoma volume was good. The hematoma volume was 29-37 (33.3 ± 1.4) μL calculated by the Coniglobus formula (A × B × C/2). No evidence of ICH was found in the control group or sham group.

EMSA

EMSA was performed to detect the NF-κB activation. The results suggested that NF-κB activation in all the ICH groups showed significant differences compared with that in the control group ($P < .01$). NF-kB activation at 2 day after ICH was significantly higher than that at 1 day ($P < .005$) and 4 day ($P < .005$). Meanwhile, that at 10 day after ICH was significantly higher than that at 7 day ($P < .005$) and 14 day ($P < .005$). Therefore, bimodal distribution was shown in the NF-κB activation, which was detected at 6 hour after ICH, reached the first peak at 2 day, then decreased and reached the second peak at 10 day, and then decreased at last (Fig 1).

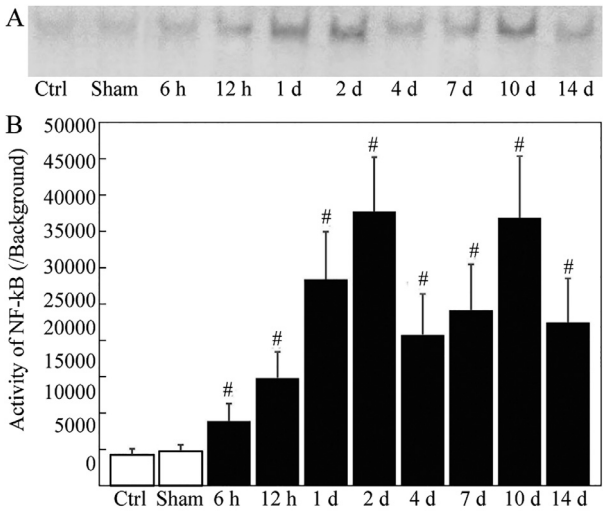

Figure 1. *Activation profiling and column chart of NF-κB detected with electrophoretic mobility shift assay (EMSA). (A) The representative EMSA result showed the NF-κB activity of the control, sham and each ICH group. (B) Column chart showed the bimodal distribution of NF-κB activation, which was detected at 6 hour after ICH, reached the first peak at 2 day, then decreased and reached the second peak at 10 day, and then decreased at last. NF-κB activation in all of the ICH groups showed significant differences compared with that in the control group. Bars represent mean ± SD (n = 8, each group),* #P<.01 *versus control group. Abbreviations: EMSA, electrophoretic mobility shift assay; ICH, intracerebral hemorrhage; NF-κB, nuclear factor.*

Western Blotting

Protein levels of 3 NF-κB subunits, including p50, p65 and c-Rel, were detected with Western blotting. The results showed that the changing trends of the 3 subunits were different from each other. P50 and p65 were expressed in the early stage of ICH. Compared with the control group, p50 and p65 expression began increasing at 6 hour after ICH, reached the peak at 1 day and 2 day, respectively, then decreased, and returned to normal at 10 day. However, c-Rel was expressed in the late stage of ICH, as it increased at 4 day after ICH, reached the peak at 10 day and then decreased (Fig 2).

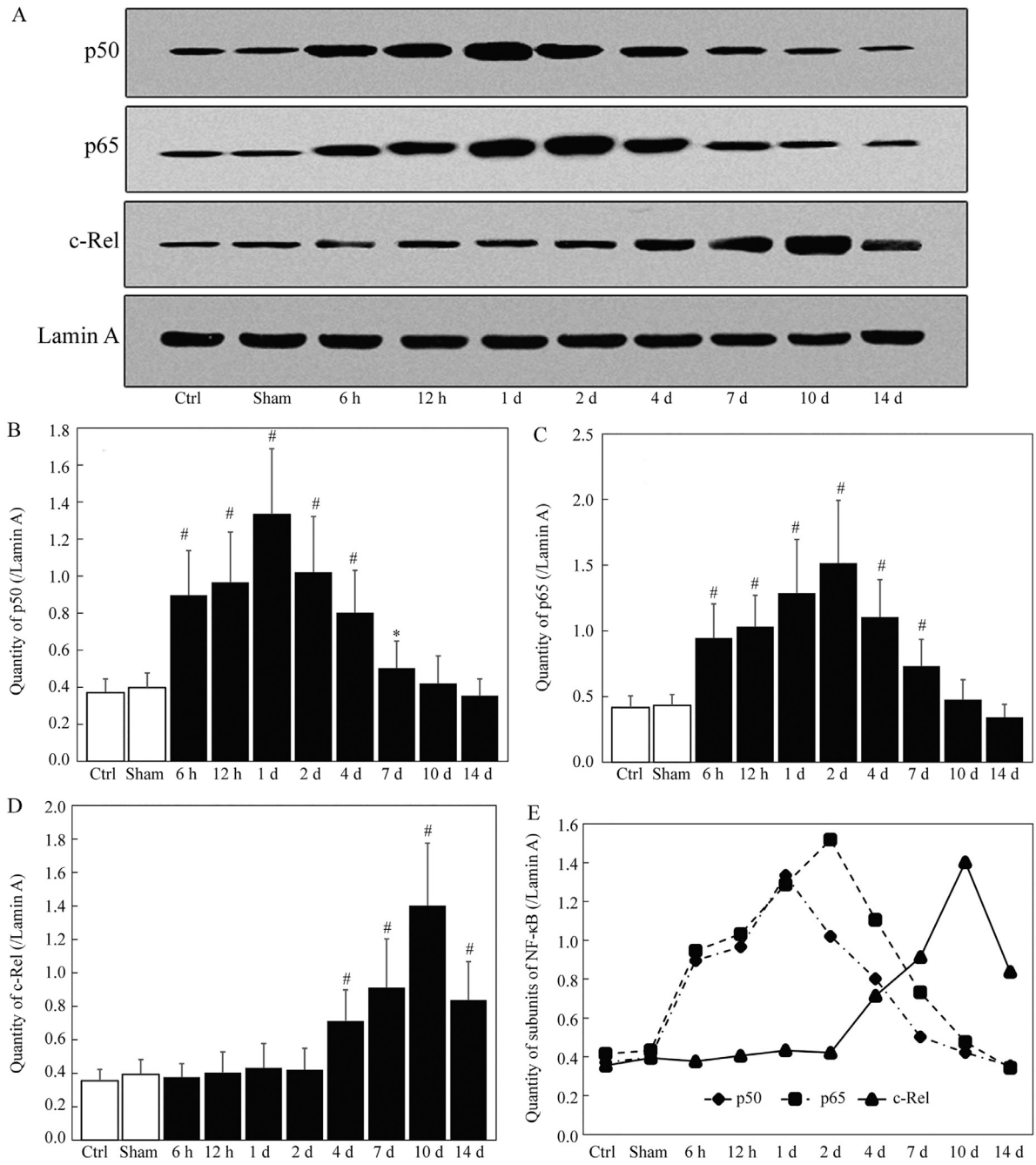

Figure 2. *Expression profiling, column chart, and line chart of NF-κB subunits in nucleoprotein, including p50, p65, and c-Rel, detected with Western blotting. (A) The representative Western blotting result showed the NF-κB subunits expression in nucleoprotein of the control, sham and each ICH group. (B, C, D, and E) Column chart and line chart showed p50 and p65 expressed in the early stage of ICH. Compared with the control group, p50 and p65 expression increased at 6 hour after ICH, reached the peak at 1 day and 2 day, respectively, then decreased, and returned to normal at 10 day. C-Rel expressed in the late stage of ICH, as it increased at 4 day after ICH, reached the peak at 10 day and then decreased. Bars represent mean ± SD (n = 8, each group), * P<0.05 vs control group, #P<0.01 versus control group. Abbreviations: ICH, intracerebral hemorrhage; NF-κB, nuclear factor.*

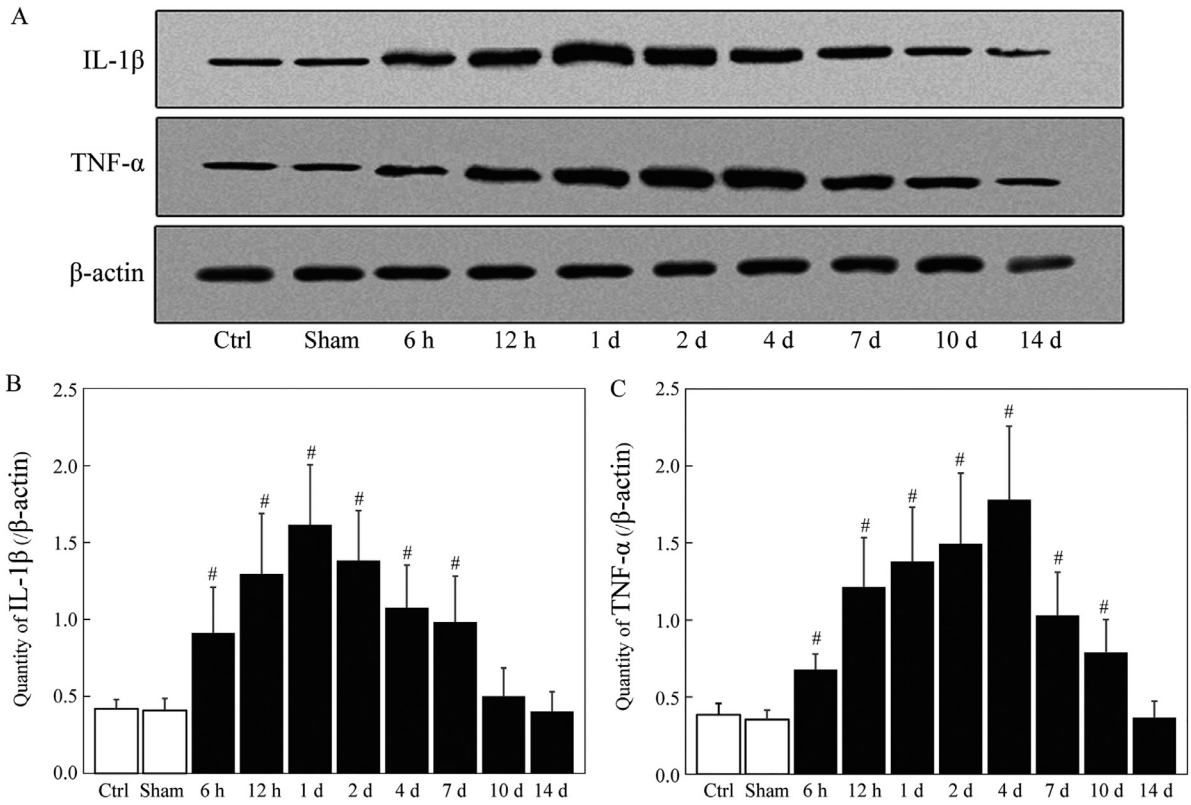

Figure 3. *Expression profiling and column chart of IL-1β and TNF-α detected with Western blotting. (A) The representative Western blotting result showed the IL-1β and TNF-α of the control, sham and each ICH group. (B, C) Column chart showed that compared with the control group, the expression of IL-1β and TNF-α increased at 6 hour after ICH, reached the peak at 1 day and 4 day, respectively, then decreased, and returned to normal at 10 day and 14 day, respectively. Bars represent mean ± SD (n = 8, each group),* $^{\#}P<0.01$ *versus control group. Abbreviations: ICH, intracerebral hemorrhage; IL-1β, interleukin-1β; TNF-α, tumor necrosis factor-α.*

Compared with the control group, the expression of IL-1β and TNF-α increased at 6 hour after ICH, reached the peak at 1 day and 4 day, respectively, then decreased, and returned to normal at 10 day and 14 day, respectively (Fig 3).

The expression of bcl-2 and caspase-3 indicated the opposite trend. The expression of bcl-2 declined at 6 hour after ICH, reached the nadir at 4 day, and returned to normal level at 10 day. But as for caspase-3, the expression increased at 6 hour after ICH, reached the peak at 2 day, then declined gradually, and returned the normal level at 10 day (Fig 4).

TUNEL Assay

Cell death was detected by the TUNEL assay. Significant differences were observed between each of the experimental group and control group. The number of TUNEL-positive cells increased at 6 hour after ICH, reached the peak at 4 day, and then decreased (Fig 5).

Discussion

The main findings of the present study were as follows: (1) NF-κB activation showed a bimodal distribution mode after ICH. The first peak was reached at 2 day, and the second at 10 day after ICH; (2) the bimodal distribution mode of NF-κB activation was due to the expression of its subunits. The expression of p50 and p65 reached the peak at 1 day and 2 day, leading to the first peak of NF-κB activation, and that of c-Rel at 10 day after ICH, leading to the second peak of NF-κB activation; (3) the expression of inflammatory factors IL-1β and TNF-α reached the peak at 1 day and 4 day, respectively; and (4) the peak of cell death and caspase-3 expression, and the nadir of bcl-2 expression appeared to be synchronizing with or right after the first peak of NF-κB activation. Then, at the second peak of NF-κB activation, cell death and caspase-3 expression decreased and the bcl-2 expression returned to the normal level.

NF-κB is regarded as the key regulator in the inflammatory response. Previous studies of human and animal models of ICH suggested that there was a close relationship among the NF-κB activation, apoptosis, and prognosis.[9,11,20-23] Some previous studies proved that NF-κB activation promoted cell death,[9,20] whereas other studies suggested the opposite.[21-23] Clemens et al[24] indicated that sustained NF-κB activation could induce nerve cell death, whereas transient activation might be neuroprotective. Therefore, there is still debate whether NF-κB activation promotes cell death or it is a compensatory mechanism to promote cell survival.

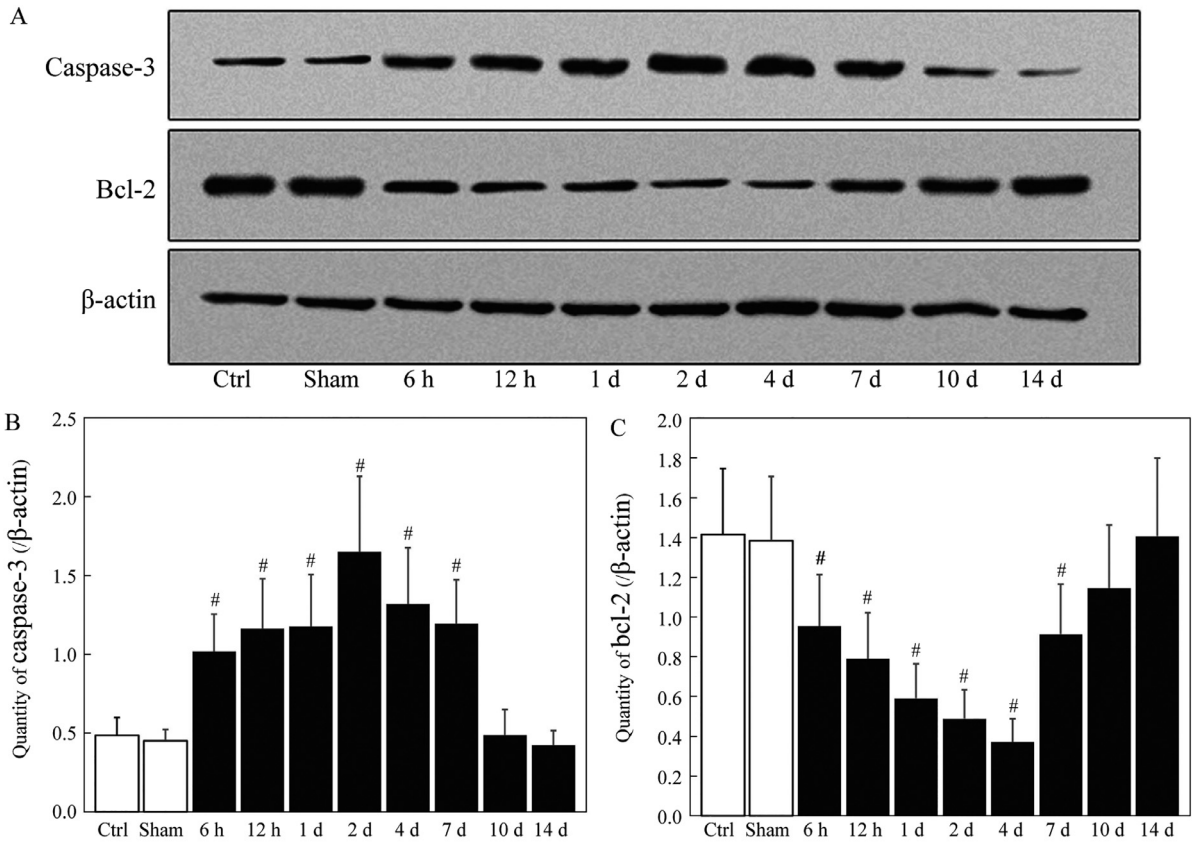

Figure 4. *Expression profiling and column chart of bcl-2 and caspase-3 detected with Western blotting. (A) The representative Western blotting showed the bcl-2 and caspase-3 of the control, sham, and each ICH group. (B and C) Column chart showed that compared with the control group, the expression of bcl-2 declined at 6 hour after ICH, reached the nadir at 4 day, and returned to normal level at 10 day. For caspase-3, the expression increased at 6 hour after ICH, reached the peak at 2 day, then declined gradually, and returned the normal level at 10 day. Bars represent mean ± SD (n = 8, each group), #P < .01 versus control group. Abbreviations: ICH, intracerebral hemorrhage.*

NF-κB comprises NF-κB 1 (p50), NF-κB 2 (p52), RelA (p65), RelB, and c-Rel subunits. Dimerization of NF-κB/Rel protein family members is required. Each of the different composition of the dimer has the following different characteristics: different affinity for the same kappa B sequence, different specificity of the induced cells, different localization in the subcellular structure, and different interaction with IκB and activity level. Therefore, the cells can differentially regulate the expression of the gene by selection of slightly different kappa B sequences and dimers with different affinity under different stimuli or different physiological states.[8,25-27]

According to the previous studies, different NF-κB subunits might be involved in different pathophysiological processes and play different roles in the disease process. Nijboer et al[16] studied the HI rat model, and found that there were 2 peaks of cerebral NF-κB activity at 3-6 and 24 hour after HI. Early NF-κB activation contributes to neonatal HI brain damage, and late NF-κB provides endogenous neuroprotection and upregulates antiapoptotic molecules. Inhibition of early NF-κB activity is neuroprotective only when late NF-κB activity is maintained. Therefore, we can speculate that the 2 peaks of NF-κB activity after HI might stem from 2 different NF-κB dimmers. However, the expression of NF-κB subunits was not detected in this study. You et al[17] studied the SAH model in vivo and in vitro. Their results suggested that biphasic increasing of NF-κB activity was induced after SAH, and the early NF-κB activity peak indicated the injury role on neurons, and the late peak might not be involved in the deteriorated effect on neurons. In the field of TBI, Hu et al[28] found that biphasic activation of NF-κB could be induced after experimental TBI in rats. NF-κB p65 and c-Rel subunits were elevated at different post-TBI time periods, leading to a hypothesis that different NF-κB subunits might be involved in different pathophysiological processes after TBI.

In the present study, NF-κB activation, expressions of subunits, inflammatory factors, and apoptosis related factors, as well as cell death were detected from the early brain injury stage to the late brain recovery stage. In the early stage, as the activation of NF-κB increased, the expression of inflammatory factors IL-1β and TNF-α increased correspondingly. As key inflammatory factors, IL-1β and TNF-α play an important role in promoting the inflammatory reaction, cerebral edema, or apoptosis after

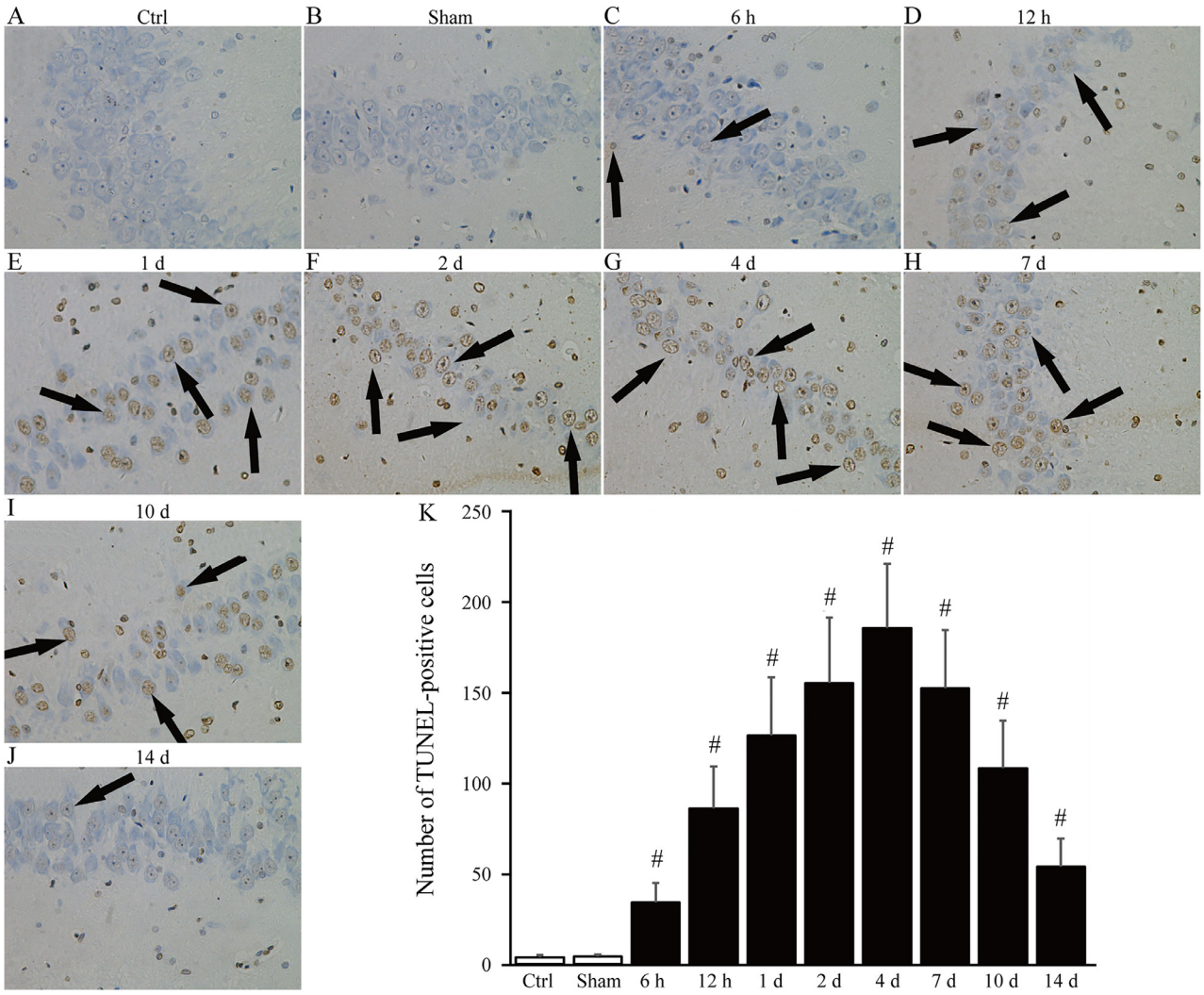

Figure 5. *Microscopic images and column chart of cell death detected with terminal deoxynucleotidyl transferase-mediated dUTP-biotin nick end labeling (TUNEL) assay. (A-J) Microscopic images (400×) of the control, sham, and each ICH group showed the TUNEL-positive cells. (K) Column chart showed that significant differences were observed between each of the experimental group and control group. The number of TUNEL-positive cells increased at 6 hour after ICH, reached the peak at 4 day, and then decreased. → indicates TUNEL-positive cells. Bars represent mean ± SD (n = 8, each group),* $^{\#}P < .01$ *versus control group. Abbreviations: ICH, intracerebral hemorrhage.*

ICH through a variety of ways.[29,30] Cell death and expression of apoptosis-related factors in the early stage also reflected the damage of brain tissue. Apoptotic cell death participates in the process of secondary brain injury after ICH.[5,23,31,32] Human and animal studies have demonstrated the close relationship between NF-κB activation and apoptotic cell death,[11,23] which is achieved through the apoptosis-related factors. The apoptosis-related factors bcl-2 and caspase-3, which are regulated by NF-κB, have the anti-apoptosis and apoptosis-promoting effects respectively. Bcl-2 has been proved to promote neuronal regeneration and survival, and have anti-apoptotic effect.[5,23,33] Caspase-3 can cleave the poly (ADP-ribose) polymerase, which is related to DNA repair and genetic integrity, into 2 fragments and have apoptosis-promoting effect.[34] In the present study, cell death and caspase-3 expression increased gradually after ICH and peaked at the first peak of NF-κB activation, whereas anti-apoptotic factor bcl-2 showed the opposite trend, indicating the first peak of NF-κB activation, that is to say p50 and p65 expression, can promote inflammatory reaction and cell death. In the late brain recovery stage, NF-κB activation and c-Rel expression reach the second peak on the 10th day, and meanwhile, the levels of IL-1β, TNF-α, cell death, and caspase-3 gradually decreased and bcl-2 also recovered to the normal range, indicating that c-Rel expression has the role of anti-apoptosis and reducing inflammation.

According to the present study, we can speculate that different subunits have different effects after ICH. P50 and p65 may promote the inflammatory response and apoptosis, and c-Rel may play the opposite role. However, the hypothesis has never been confirmed for ICH and any other field, such as SAH, TBI, and HI. This is also the

limitation of this study. To clarify these issues, further studies will be conducted soon in our research center. Drug (inhibiting or promoting NF-κB activation) intervention, RNA interference and gene overexpression will be performed at the different phases after ICH. The results of the present study can provide important evidence to the feasibility of further studies. Meanwhile, the time of the intervention in further studies will also be defined according to the NF-κB activation variations in the present study.

Conclusions

In summary, in the current study we found that NF-κB activation showed a bimodal distribution mode after ICH. We can speculate that different subunits have different effects after ICH. P50 and p65 may promote the inflammatory response and apoptosis, and c-Rel may play the opposite role. Measures might be performed at the different phases to reduce the brain injury in the early stage and promote the brain recovery in the late stage after ICH.

Competing Interests

The authors declare that they have no competing interests.

References

1. Narayan SK, Sivaprasad P, Sushma S, et al. Etiology and outcome determinants of intracerebral hemorrhage in a south Indian population, a hospital-based study. Ann Indian Acad Neurol 2012;15:263-266.
2. Qureshi AL, Tuhrim S, Broderick JP, et al. Spontaneous intracerebral hemorrhage. N Engl J Med 2001;344:1450-1460.
3. Tsai CF, Thomas B, Sudlow CL. Epidemiology of stroke and its subtypes in Chinese vs white populations: a systematic review. Neurology 2013;81:264-272.
4. Zhao XR, Gonzales N, Aronowski J. Pleiotropic role of PPARγ in intracerebral hemorrhage: an intricate system involving Nrf2, RXR, and NF-κB. CNS Neurosci Ther 2015;21:357-366.
5. Bobinger T, Burkardt P, Huttner HB, et al. Programmed cell death after intracerebral hemorrhage. Curr Neuropharmacol 2018;16:1267-1281.
6. Xi G, Keep RF, Hoff JT. Mechanisms of brain injury after intracerebral haemorrhage. Lancet Neurol 2006;5:53-63.
7. Barnes PJ, factor-kappaB KMar. A pivotal transcription factor in chronic inflammatory diseases. N Engl J Med 1997;336:1066-1071.
8. Miraghazadeh B, Cook MC. Nuclear factor-kappaB in autoimmunity: man and mouse. Front Immunol 2018;9:613.
9. Ridder DA, Schwaninger M. NF-κB signaling in cerebral ischemia. Neuroscience 2009;158:995-1006.
10. Yin M, Chen Z, Ouyang Y, et al. Thrombin-induced, TNFR-dependent miR-181c downregulation promotes MLL1 and NF-κB target gene expression in human microglia. J Neuroinflammation 2017;14:132.
11. Zhang ZL, Liu YG, Huang QB, et al. NF-κB activation and cell death after intracerebral hemorrhage in patients. Neurol Sci 2014;35:1097-1102.
12. Zhang ZL, Liu YG, Huang QB, et al. Nuclear factor-κB activation in perihematomal brain tissue correlates with outcome in patients with intracerebral hemorrhage. J Neuroinflammation 2015;12:53.
13. Zhang Y, Chen Y, Wu J, et al. Activation of dopamine D2 receptor suppresses neuroinflammation through αB-Crystalline by inhibition of NF-κB nuclear translocation in experimental ICH mice model. Stroke 2015;46:2637-2646.
14. Youssef S, Steinman L. At once harmful and beneficial: the dual properties of NF-kappaB. Nat Immunol 2006;7:901-902.
15. Pizzi M, Goffi F, Boroni F, et al. Opposing roles for NF-kappaB/Rel factors p65 and c-Rel in the modulation of neuron survival elicited by glutamate and interleukin-1beta. J Biol Chem 2002;277:20717-20723.
16. Nijboer CH, Heijnen CJ, Groenendaal F, et al. A dual role of the NF-kappa B pathway in neonatal hypoxic-ischemic brain damage. Stroke 2008;39:2578-2586.
17. You WC, Li W, Zhuang Z, et al. Biphasic activation of nuclear factor-kappa B in experimental models of subarachnoid hemorrhage in vivo and in vitro. Mediators Inflamm 2012;2012:786242.
18. Chu K, Jeong SW, Jung KH, et al. Celecoxib induces functional recovery after intracerebral hemorrhage with reduction of brain edema and perihematomal cell death. J Cereb Blood Flow Metab 2004;24:926-933.
19. Jung KH, Chu K, Jeong SW, et al. HMG-CoA reductase inhibitor, atorvastatin, promotes sensorimotor recovery, suppressing acute inflammatory reaction after experimental intracerebral hemorrhage. Stroke 2004;35:1744-1749.
20. Hu YY, Huang M, Dong XQ, et al. Ginkgolide B reduces neuronal cell apoptosis in the hemorrhagic rat brain: possible involvement of Toll-like receptor 4/nuclear factor-kappa B pathway. J Ethnopharmacol 2011;137:1462-1468.
21. Song YS, Lee YS, Narasimhan P, et al. Reduced oxidative stress promotes NF-κB-mediated neuroprote ctive gene expression after transient focal cerebral ischemia: lymphocytotrophic cytokines and antiapoptotic factors. J Cereb Blood Flow Metab 2007;27:764-775.
22. Bhakar AL, Tannis LL, Zeindler C, et al. Constitutive nuclear factor-kappa B activity is required for central neuron survival. J Neurosci 2002;22:8466-8475.
23. Shen X, Ma L, Dong W, et al. Autophagy regulates intracerebral hemorrhage induced neural damage via apoptosis and NF-κB pathway. Neurochem Int 2016;96:100-112.
24. Clemens JA, Stephenson DT, Yin T, et al. Drug-induced neuroprotection from global ischemia is associated with prevention of persistent but not transient activation of nuclear factor-κB in rats. Stroke 1998;29:677-682.
25. Mercurio F, Zhu H, Murray BW, et al. IKK-1 and IKK-2: Cytokine-activated IκB kinases essential for NF-κB activation. Science 1997;278:860-866.
26. Hayden MS, Ghosh S. Signaling to NF-kappaB. Genes Dev 2004;18:2195-2224.
27. Mattson MP, Meffert MK. Roles for NF-kappaB in nerve cell survival, plasticity, and disease. Cell Death Differ 2006;13:852-860.
28. Hu YC, Sun Q, Li W, et al. Biphasic activation of nuclear factor kappa B and expression of p65 and c-Rel after traumatic brain injury in rats. Inflamm Res 2014;63:109-115.
29. Holmin S, Mathiesen T. Intracerebral administration of interleukin-1β and induction of inflammation, apoptosis, and vasogenic edema. J Neurosurg 2000;92:108-120.
30. Denes A, Pinteaux E, Rothwell NJ, et al. Interleukin-1 and stroke: biomarker, harbinger of damage, and therapeutic target. Cerebrovasc Dis 2011;32:517-527.

31. Wu Z, Zou X, Zhu W, et al. Minocycline is effective in intracerebral hemorrhage by inhibition of apoptosis and autophagy. J Neurol Sci 2016;371:88-95.
32. Zhou F, Liu Y, Yang B, et al. Neuroprotective potential of glibenclamide is mediated by antioxidant and anti-apoptotic pathways in intracerebral hemorrhage. Brain Res Bull 2018;142:18-24.
33. Yuan DM, Shen JH, Yan YH, et al. Upregulated expression of SSTR1 is involved in neuronal apoptosis and is coupled to the reduction of bcl-2 following intracerebral hemorrhage in adult rats. Cell Mol Neurobiol 2014;34:951-961.
34. Sun DB, Xu MJ, Chen QM, et al. Significant elevation of serum caspase-3 levels in patients with intracerebral hemorrhage. Clin Chim Acta 2017;471:62-67.